MODELING THE VISCOPLASTIC BEHAVIOR OF INCONEL 718 AT 1200°F

M.S. Abdel-Kader†, J. Eftis, and D.L. Jones
School of Engineering and Applied Science
The George Washington University
Washington, D.C. 20052

Inconel 718 is a nickle-based superalloy that possesses several outstanding elevated-temperature mechanical properties. It has been widely used for the manufacture of critical compressor and turbine engine components requiring relatively long service lives. A large number of tests, including tensile, creep, fatigue, and creep-fatigue have been performed to characterize the mechanical properties of Inconel 718 at 1200°F, the operating temperature for turbine blades. In addition, a few attempts have been made to model the behavior of Inconel 718 at 1200°F using viscoplastic theories.

The Chaboche theory of viscoplasticity can model a wide variety of mechanical behavior, including monotonic, sustained, and cyclic responses of homogeneous, initially-isotropic, strain-hardening (or softening) materials. It has been successfully used to model the viscoplastic behavior of several structural materials of practical importance. This paper shows how the Chaboche theory can be used to model the viscoplastic behavior of Inconel 718 at 1200°F. First, an algorithm has been developed to systematically determine the material parameters of the Chaboche theory from uniaxial tensile, creep, and cyclic data. The algorithm, however, is general and can be used in conjunction with similar high-temperature materials. A sensitivity study was then performed and an 'optimal' set of Chaboche's parameters was obtained. This study has also indicated the role of each parameter in modeling the response to different loading conditions. Based on the 'optimal' set of material parameters, uniaxial tensile, creep, and cyclic behavior has been predicted. The results were compared to available experimental data and the agreement was found to be good. Moreover, predicted behavior of Inconel 718 at 1200°F under a variety of additional loading conditions has been examined and relevant conclusions were drawn.

I. INTRODUCTION

For high temperature applications, such as those encountered in the nuclear and aerospace industries, severe demands are generally placed on candidate structural materials. These demands have led to the development of a new class of structural materials called superalloys having considerably improved elevated-temperature mechanical properties. One such material is Inconel 718, which possesses several excellent properties such

† On leave from The Military Technical College, Cairo, Egypt.

as creep-rupture strength, high-cycle fatigue strength, oxidation resistance, and long time stability [1-3]. These properties are, for the most part, due to the susceptibility of this material to precipitation hardening and strengthening caused by coherent gamma prime precipitates. These properties can be obtained by two different solution annealing and aging procedures. A comparative study of the effects of both types of heat treatment procedures on the tensile and fatigue behavior of Inconel 718 from room temperature to 1200°F has been presented in Ref. [2]. It was concluded that Inconel 718 subjected to the so called 'standard heat treatment' exhibits higher resistance to stress rupture and fatigue. Therefore, Inconel 718 in this condition is widely used in current production of gas turbine engine components requiring relatively long service lives and operating normally at high temperatures [1,4].

A large number of uniaxial monotonic, sustained, and cyclic tests have been performed to obtain the mechanical properties of Inconel 718 at 1200°F [1-9]. However, only a few of these tests address the strain-rate sensitivity, with the result that no significant strain rate sensitivity could be observed for $\dot{\epsilon} > 5\text{x}10^{-5}$ sec^{-1}. At lower strain rates, tensile and cyclic data were too limited to establish the rate sensitivity of this material, although existing creep data do suggest the existence of some rate sensitivity.

Domas, et al [4] have shown that the tensile and stabilized cyclic stress-inelastic strain curves for Inconel 718 at 1200°F can be described by the Ramberg-Osgood form

$$\sigma = K^* (\epsilon'')^{n^*}, \qquad (1)$$

where σ and ϵ'' are the tensile stress and inelastic strain (or the stress at the tensile tip of the stabilized hysteresis loop and the corresponding inelastic strain amplitude), respectively, and K^* and n^* are material parameters that depend on the heat treatment and strain rate. Values of K^* and n^* for Inconel 718 (standard heat treatment) at 1200°F and for different tensile and cyclic strain rates are listed in Table 1. The first five sets of values were determined by Domas, et al [4], whereas the remaining values were determined within a larger study [10], part of which is the present

work. Available experimental data on the cyclic behavior of Inconel 718 at 1200°F have also indicated that this material cyclically softens for approximately 10-20% of its fatigue life, followed by a period of near-stabilization when damage mechanisms are activated. For convenience the values of σ and $\epsilon^{"}$ used to evaluate the cyclic material parameters in Table 1 were those at $N_f/2$, where N_f is the fatigue life.

Inconel 718 at 1200°F displays classical creep response (primary, secondary, and tertiary creep stages). The time to the onset of tertiary creep is normally about 0.5 t_r, where t_r is the rupture life [11]. For Inconel 718, however, the region of increasing creep rates following steady state creep commences at about 0.3 t_r [3]. This suggests that the initiation of increasing creep rates may be due to softening and is not necessarily a manifestation of the instability associated with tertiary creep [3,6]. Thus, from a unified viscoplastic theory view-point, some provision for softening (or increasing creep rates) must be incorporated into the theory. Booker [3,6] has developed a creep model in the form

$$\epsilon_n = \text{EXP}\,[1.75(t_n - 1)] \cdot t_n^{0.2}, \qquad 0 < t_n < 1, \tag{2}$$

which describes the salient features of the creep behavior of Inconel 718 at 1200°F. In Eq. (2), $\epsilon_n = \epsilon/\epsilon_{tr}$ is the normalized creep strain, $t_n = t/t_{tr}$ is the normalized time; provided that ϵ_{tr} and t_{tr} are the strain and time to tertiary creep given empirically by

$$t_{tr} = 0.392\ t_r^{1.04}, \tag{3}$$

$$\epsilon_{tr} = 0.2 + 1.16\ t^{-0.14} \cdot \tag{4}$$

The time to failure, t_r, is given by

$$\log t_r = 163.92 + 23924/T - 226.92 \log \sigma_h + 94.196\ (\log \sigma)^2 - 13.215\ (\log \sigma)^3, \tag{5}$$

where T is the temperature in ^{o}K and σ_h is the hold stress in MPa. In Eqs. (2) thru (5), time is given in hours and strain in percent.

A few attempts have been made to model the behavior of Inconel 718 at $1200^{o}F$ using unified viscoplastic theories, e.g., [7,8]. In this paper, the Chaboche yield-based theory of viscoplasticity [12,13] is used for the same purpose. This theory can model a wide variety of rate-dependent inelastic mechanical behavior, including monotonic, sustained, and cyclic responses. It also models isotropic and kinematic strain hardening, including cyclic hardening (or softening) and the multidimensional Bauschinger effect. This theory has been employed to model the mechanical response of Inconel 100 [12,14], type 316 stainless steel [15,16], and Ti-6Al-4V alloy [17,18]. However, the theory does not account for the rate dependence of initial yield, which limits its use to materials that do not exhibit such behavior within the loading rates of interest. In a previous paper [19], the authors have shown how rate dependency of initial yielding can be incorporated into the Chaboche theory, without changing its general structure. The principal objective of the current paper is to show how the extended theory can be used to model the mechanical behavior of Inconel 718 at $1200^{o}F$. A major part of this effort has been devoted to developing a systematic algorithm for the determination of the Chaboche material parameters from available uniaxial test data. The need for a systematic procedure for determining the material parameters of a viscoplastic theory from the results of standard mechanical tests has been addressed [17,21].

A sensitivity study was then undertaken to explore the effects of introducing small changes in the Chaboche material parameters on different predictions and to obtain an 'optimal' set of the material parameters that globally improves the predicted behavior. The 'optimal' set was then incorporated into the Chaboche set of differential equations; and uniaxial tensile, creep, and cyclic responses were predicted and compared to available experimental data. In addition, strain-rate and strain-rate-history effects, creep, stress relaxation, and the load-unload-reload effects were predicted and examined.

II. CONSTITUTIVE EQUATIONS

In the present paper, the one-dimensional form of the Chaboche theory is presented and used; the three-dimensional form of the theory can be found elsewhere [12,13]. A basic assumption of the theory is the decomposition of the rate of deformation into rate-independent elastic and rate-dependent inelastic components. For infinitesimal deformations, the strain rate, $\dot{\epsilon}$, approximates the rate of deformation, or

$$\dot{\epsilon} = \dot{\epsilon}' + \dot{\epsilon}'' \,. \tag{6}$$

The linear elastic strain rate, $\dot{\epsilon}'$, is obtained from the time derivative of Hooke's law, that is,

$$\dot{\epsilon}' = \dot{\sigma}/E \tag{7}$$

where σ is the stress and E is Young's modulus. The nonlinear inelastic strain rate, $\dot{\epsilon}''$, is based on the normality hypothesis and has the form

$$\dot{\epsilon}'' = \begin{cases} \left(\frac{F}{K}\right)^n \, Sg(\sigma - Y), & F > 0, \\ 0, & F \leq 0, \end{cases} \tag{8}$$

where K and n are material parameters. F is the von Mises yield function given by

$$F(\sigma, Y, p) = |\sigma - Y| - R(p), \tag{9}$$

where Y is the kinematic hardening variable, p is the cumulative inelastic strain defined in terms of the inelastic strain rate by

$$p = \int_0^t |\dot{\epsilon}''| \, d\tau, \tag{10}$$

and R is the isotropic hardening variable associated with p. Note that in Chaboche's theory, as in most of the viscoplastic theories, two variables, Y

and p, are employed to model hardening. Note also that F represents the overstress, whose positive values signify the initiation of inelastic deformations [c.f. Eq. (8)].

The evolution of the kinematic hardening variable is given by

$$\dot{Y} = c(a\dot{\epsilon}^{n} - Y\dot{p}) - \gamma|Y|^{m} Sg(Y), \tag{11}$$

where c,a,γ, and m are material parameters. The first term on the right hand side of Eq. (11) is the nonlinear Armstrong-Frederick modification of Prager's linear kinematic hardening rule, which is appropriate for cyclic loading. The second term models softening effects such as reduced hardening rate, secondary creep, and stress relaxation typically associated with elevated temperatures. Equation (11) provides an effective tool by which anisotropic hardening (Bauschinger effect) and creep/relaxation effects can be appropriately modeled and represents one of the principal advantages of the Chaboche theory. In its modified form [19], the isotropic hardening variable, R, depends on the cumulative inelastic strain, p, and the total strain rate, $\dot{\epsilon}$, rather than on p alone, as postulated in the original theory. The dependence of R on $\dot{\epsilon}$ is assumed to be limited to its initial value, R_o, that is,

$$R(p,\dot{\epsilon}) = q + [R_o(\dot{\epsilon}) - q]\, e^{-bp}, \tag{12}$$

where b and q are material parameters and R_o is the rate-dependent initial yield strength.

III. DETERMINATION OF THE CHABOCHE MATERIAL PARAMETERS

In its modified form, the Chaboche theory incorporates eight viscoplastic material parameters and the rate-dependent initial yield strength [c.f. Eqs. (8), (11), and (12)], which are generally temperature-dependent. It is now shown how these parameters as well as the function $R_o(\dot{\epsilon})$ were determined from available experimental data of Inconel 718 at 1200°F. Some approximations and assumptions had to be made; these will be discussed as they are introduced.

Determination of a and c

The Chaboche flow law given by Eqs. (8) and (9), upon inversion, takes the form

$$\sigma = Y + R + K(\dot{\epsilon}")^{1/n} \quad . \tag{13}$$

At relatively high strain rates, the recovery term in Eq. (11) can be neglected, thereby allowing it to be integrated as

$$Y = sa + (Y_o - sa)\, e^{-sc(\epsilon"-\epsilon"_o)} \quad , \tag{14}$$

where

$$s = Sg(\dot{\epsilon}") = \begin{cases} +1, & \dot{\epsilon}" > 0, \\ -1, & \dot{\epsilon}" < 0, \end{cases} \tag{15}$$

and Y_o and $\epsilon"_o$ are the initial values of Y and $\epsilon"$.

For the stabilized cycle of a strain-controlled cyclic test, R assumes its saturation value q [c.f Eq. (12)], whereas Y alternates between two extreme values, Y_{max} and $Y_{min} = -Y_{max}$. It can be shown that [10,12]

$$Y_{max} = a(1 - e^{-c\Delta\epsilon"})/(1 + e^{-c\Delta\epsilon"}) = a \tanh(c\epsilon"_a) \quad , \tag{16}$$

where $\epsilon"_a = \Delta\epsilon"/2$ is the stabilized inelastic strain amplitude. Hence, if a series of stain-controlled cyclic tests are performed until stabilization has occurred, a cyclic stress-strain curve can be established through the tensile peaks of these stabilized hysteresis loops. Such a curve, within the context of Chaboche's theory, can be represented by use of Eqs. (13) and (16) as

$$\sigma = a \tanh(c\epsilon"_a) + q + K(\dot{\epsilon}")^{1/n} \quad , \tag{17}$$

which, when differentiated with respect to $\epsilon"_a$, yields

$$d\sigma/d\epsilon"_a = a\, c\, \mathrm{sech}^2(c\epsilon"_a) \quad . \tag{18}$$

An alternative form for Eq. (18) can also be obtained by differentiating Eq. (1), i.e.,

$$d\sigma/d\epsilon_a'' = n^*K^*(\epsilon_a'')^{n^*-1} \cdot \tag{19}$$

Since values of K^* and n^* are available (c.f. Table 1), Eq. (19) can be used to generate values of $f_i = d\sigma/d\epsilon_a''$ for $(\epsilon_a'')_i$, i=1,2,...,n. These values can be used to evaluate a and c in Eq. (18). This is, in fact, a nonlinear regression analysis problem. Draper and Smith [22] have shown how such a problem can be solved based on the least squares technique. A computer program based on their analysis has been developed and used to find the values of a and c listed in Table 1. The first and seventh sets are considerably different from the remaining values. Therefore, these two sets were excluded and mean values of a and c were calculated for the remaining sets as

$$a = 31.40 \text{ KSI}, \qquad c = 349.5 \cdot \tag{20}$$

Determination of K and n

Since the material parameters K and n characterize the rate dependency of the material response, they were evaluated from tensile data at different strain rates. Two tensile stress-strain curves may be adequate for this purpose. Figure 1 illustrates two stress-strain curves at strain rates of $\dot{\epsilon}_1$ and $\dot{\epsilon}_2$, where $\dot{\epsilon}_2 > \dot{\epsilon}_1$. If it is assumed that these rates are sufficiently high and close together, then Eq. (14) holds for Y, and R_o can be considered the same for both cases. Thus,

$$Y_{a_1} = Y_{a_2}, \quad Y_{b_1} = Y_{b_2}, \quad R_{a_1} = R_{a_2}, \quad R_{b_1} = R_{b_2}, \tag{21}$$

where a_1, a_2, b_1, and b_2 are shown in Fig. 2.

From Eqs. (13) and (21), the stress differential may be written as

$$\Delta\sigma_a = \sigma_{a_2} - \sigma_{a_1} = K\left[(\dot{\epsilon}_{a_2}'')^{1/n} - (\dot{\epsilon}_{a_1}'')^{1/n}\right], \tag{22}$$

which relates the difference in stress levels to the corresponding inelastic strain rates at specific inelastic strain values. It is necessary, therefore, to evaluate the inelastic strain rate at different points on both curves using the equation

$$\dot{\epsilon}'' = \dot{\epsilon} - \dot{\epsilon}' = \dot{\epsilon} - \dot{\sigma}/E = \dot{\epsilon} - \dot{\epsilon}\left(\frac{d\sigma}{d\epsilon}\right)/E = \dot{\epsilon}(1 - E^*/E), \tag{23}$$

where $E^* = d\sigma/d\epsilon$ is the instantaneous slope of the stress-strain curve. Equation (1), along with the integrated form of Eq. (6), can be employed to obtain the relation

$$\frac{d\epsilon}{d\sigma} = \frac{1}{E} + \frac{1}{n^*K^*}\left(\frac{\sigma}{k^*}\right)^{\frac{1}{n^*} - 1} . \tag{24}$$

Note that the inverse of this equation is E^*. Therefore, Eqs. (23) and (24) can be used to calculate values of $\dot{\epsilon}''_{a_1}$ and $\dot{\epsilon}''_{a_2}$ in Eq. (22), and $\Delta\sigma_a$ can be obtained by applying Eq. (1) independently to curve 1 and curve 2 of Fig. 1. Then, K and n in Eq. (22) are evaluated using a nonlinear regression procedure similar to that used in evaluating a and c. The tensile data of Table 1 were used for this purpose, and the following values of n and K were obtained

$$n = 5.12, \qquad K = 154.4 \text{ KSI } \sqrt[n]{\text{sec}} . \tag{25}$$

Determination of b and q

Once a, c, n, and K have been obtained, b and q can be determined from the results of one strain-controlled cyclic test, such as that reported in Refs. [7,9] at $|\dot{\epsilon}| = 2.667\text{x}10^{-3}$ sec^{-1} and $\epsilon = \pm 1\%$. At the tensile tip of a hysteresis loop, Eqs. (13) and (16) can be combined and solved for R as

$$R = \sigma - a \tanh(c\epsilon''_a) - K(\dot{\epsilon}'')^{1/n}, \tag{26}$$

and p can be calculated from

$$p_n = \epsilon''_1/2 + 2\sum_{i=2}^{n} \Delta\epsilon''_i , \tag{27}$$

where n represents the n-th cycle and $\Delta\epsilon_i''$ represents the inelastic strain range at the i-th cycle. Equations (26) and (27) were then used to calculate R and p values from the strain-controlled test discussed above, with the results given in Table 2. In these calculations the overstress, $K(\dot{\epsilon}'')^{1/n}$, was assumed to be constant, since the slopes of the loops at their peaks were relatively constant. The value of $\dot{\epsilon}''$ was calculated from Eq. (23) to be 2.465×10^{-3} sec^{-1}, from which the overstress was determined to be 47.73 KSI. Since the available results did not include records of all hysteresis loops, it was assumed that a missing loop had the same value of $\Delta\epsilon''$ as the first preceding available loop. Table 2 shows that R had essentially saturated by the 32nd cycle. The corresponding value of R was, therefore, taken to be the saturation value, i.e.,

$$q = 18.63 \quad \text{KSI} \quad . \tag{28}$$

A value for b was then determined from the slope of the line

$$\ln(R-q) = \ln(R_o-q) - bp, \tag{29}$$

to be

$$b = 4.679 \quad . \tag{30}$$

Determination of R_o

In a previous paper [19], the authors have shown how the Chaboche theory can be modified to account for the rate-dependent initial yield response and permit prediction of creep behavior at low stress levels. In effect, the function $R_o(\dot{\epsilon})$ in Eq. (12) had to be evaluated. Based on the analogy between tensile and creep responses [23] and the creep data base of Ref. [8], a form for $R_o(\dot{\epsilon})$ was selected as

$$R_o = R_{oo} \left\{1 + \ln\left\{1 + \text{EXP}\left[\sum_{i=0}^{3} \alpha_i (\ln\dot{\epsilon})^i\right]\right\}\right\} , \tag{31}$$

where R_{oo}=q=18.63 KSI, α_o=25.56, α_1=4.551, α_2=0.3360, and $\alpha_3=0.8375\times10^{-2}$, as shown in Ref. [19].

Booker's creep model [c.f. Eqs. (2-5)] was used to evaluate the strain at the initiation of steady-state creep needed for these calculations. This was achieved by differentiating Eq. (2) twice with respect to time, equating to zero, solving for t_n, and then substituting back into Eq. (2) to obtain the required strain values.

Determination of m and γ

It has been shown in Ref. [17] that hardening is mostly kinematic during primary creep, because of the relatively high value of the ratio of the hardening exponents c and b [c.f. Eqs. (12) and (13)], and because of the small amount of inelastic strains that are likely to have accumulated. Therefore, it can be assumed that $R = R_o$ = constant at the attainment of steady-state creep. During secondary creep, $\dot{\epsilon} = \dot{\epsilon}''$ = constant, and the time derivative of Eq. (13) reduces to

$$\dot{Y} = c(a-Y)\,\dot{\epsilon}_{ss} - \gamma\, Y^m = 0, \tag{32}$$

where $\dot{\epsilon}_{ss}$ is the steady-state creep rate. Equation (32) can also be written as

$$\ln[c(a-Y)\,\dot{\epsilon}_{ss}] = m\,\ln Y + \ln\gamma, \tag{33}$$

which represents a straight line whose slope is m and intercept is $\ln\gamma$. In this equation, Y can be calculated from Eq. (13) with $R = R_o$. The data of Ref. [8] for small creep stresses, where the recovery effects are significant, were used to evaluate γ and m as

$$\gamma = 0.4\times10^{-10}\ , \qquad m = 6.942\ . \tag{34}$$

To conclude, a procedure has been developed to evaluate the material parameters of the modified Chaboche theory of viscoplasticity from uniaxial tensile, creep, and cyclic test data. Since these tests were not specifically designed for the purpose of determining the Chaboche parameters, the procedure employed herein to determine these parameters is not unique, but appropriate for the kind of data available. However, the procedure is general and can be employed to determine the Chaboche

parameters for any similar material. Values of the parameters are listed in Table 3. Based on these values, predictions of a tensile test at $\dot{\epsilon} = 1.333 \times 10^{-5} sec^{-1}$, a creep test at 130 KSI, and a strain-controlled, fully-reversed cyclic test at $|\dot{\epsilon}| = 4 \times 10^{-5} sec^{-1}$ and $\Delta\epsilon = 2\%$ are shown in Figs. 2 to 4, respectively, along with available experimental data for comparison.

IV. SENSITIVITY STUDY

Although the predicted and actual responses are in reasonable agreement, it was anticipated that better agreement could be achieved by modifying the parameter values. Therefore, a parametric study was undertaken to explore the sensitivity of each of the parameters to the overall predicted behavior of Inconel 718 at 1200°F, and thus lead to the determination of an 'optimal' modeling of overall material response. To perform such a multi-parameter optimization, it is necessary to have a complete and accurate set of experimental results of specific base-line tests. These tests should be chosen in such a way that all aspects of material behavior to be modeled by the theory are represented in the test data. Such a data set is not available for Inconel 718 at 1200°F, partly because of the expense of such testing, but also because existing test data were not acquired for the purpose of evaluating Chaboche's model. Therefore, it has been necessary to work with available data sets that are not adequate for the present purpose.

With this in mind, the data base of Ref. [8], which consists of tensile and creep test results only was employed to perform the parametric study. Then this data base was enlarged by including cyclic data from Ref. [4]. The first step of the parametric study consisted of varying the parameters, one at a time, by $\pm 7\%$ of the value listed in Table 3, predicting the corresponding material responses, and comparing these predictions with the selected data base. Because of space limitations, only representative samples of the results of this step are shown in Tables 4 to 6 , along with corresponding experimental data. A thorough examination of the results of this step of the parameteric study has led to the following observations:

(a) Some parameters have stronger effects on material behavior than others, in decreasing order, R_o, n, k, and m have the strongest effects.

(b) Whereas a material parameter or a subset of the parameters has a strong effect on a certain facet of material behavior, it does not necessarily have the same effect on a different aspect of material behavior. For instance, R_o had a strong effect on the creep behavior; however, it had less effect on the tensile and cyclic behavior.

(c) Creep response seems to be the most sensitive to changes in parameter values. For instance, changing R_o by $\pm 7\%$ results in approximately one order-of-magnitude change in the minimum creep rate value.

(d) Increases in b, γ, and m increase the minimum creep rate and the inelastic strain range, and decrease the saturation stress, whereas the other remaining parameters have the opposite influence.

Based on these observations, it was decided to extend the parametric study for the parameters that strongly affect the material behavior by reducing the amount of change from $\pm 7\%$ to $\pm 3.5\%$ for n, K, and m and to ± 5.25, 3.5, and 1.75% for R_o, since it seemed to be the most influential. Representative results of these changes are also included in Tables 4 to 6. These results support the previous observations in that they confirm that the overall material behavior is most sensitive to variations of R_o. For example, a change of $\pm 1.75\%$ in R_o changes the minimum creep rate by about 50 to 100%. Thus, the results of the current parametric study verify that the modification introduced to Chaboche's theory, i.e., considering R_o to be a function of the strain rate, is of critical importance for improving the accuracy of this theory.

Although the results of this parametric study have shown that the cyclic material response (first cycle $\Delta\sigma$ and $\Delta\epsilon$") is not strongly affected by small changes in b and q, the influence of these parameters is best exhibited by studying the complete cyclic behavior and not just the first cycle. Unfortunately, the only cyclic test available for this material is the one previously used to determine values of b and q. This test was conducted at $|\dot{\epsilon}| = 2.667 \times 10^{-3}$ sec^{-1}, a value which is well above the limit of rate sensitivity for Inconel 718 at $1200^{o}F$ - estimated to be about 4×10^{-5} sec^{-1}. Thus the results of such a test should not be used to determine the material parameters. Problems also arise in attempting to use Chaboche's theory to predict a rate-insensitive response, since it is basically a rate-dependent plasticity theory. This problem was demonstrated by predicting

the cyclic behavior at $|\dot{\epsilon}| = 2.667\text{x}10^{-3}$ sec^{-1} and $\epsilon = \pm 1\%$ for the first several cycles. The results showed that the stress was initially overstimated and the inelastic strain was underestimated. Also, the predicted cycles softened at a higher rate than actually observed, which suggests that b and q must be re-evaluated.

To best accomplish such a task, the hysteresis loops from a cyclic test at $|\dot{\epsilon}| \leq 4\text{x}10^{-5}$ sec^{-1} are needed. Such data, however, are not available*, and it was hypothesized by virtue of the material rate insensitivity for $\dot{\epsilon} > 4\text{x}10^{-5}$ sec^{-1} that the results of a cyclic test at $|\dot{\epsilon}| = 2.667\text{x}10^{-3}$ sec^{-1} are essentially the same as a test at $|\dot{\epsilon}| = 4\text{x}10^{-5}$ sec^{-1}. In effect, values of R have been recalculated and the new estimates of the material parameters b and q were found to be

$$b = 3.75, \qquad q = 50 \text{ KSI} \cdot \tag{35}$$

It was also found that by rounding off the values of a, c, K, m, and n, i.e.,

$$a \to 30 \text{ KSI}, \; c \to 350, \; K \to 155 \text{ KSI}\sqrt[n]{\text{sec}}, \; m \to 7, \; n \to 5.1, \tag{36}$$

insignificant effects on the predicted behavior were observed. Therefore, these values will be considered in the remainder of this work to be the 'optimal' values.

The final step in the optimization procedure was to change the form for $R_o(\dot{\epsilon})$ such that the best possible agreement could be obtained between experimental and predicted behavior. First the values of R_o that gave best prediction of overall behavior were determined and are shown in Ref. [19]. Then, an improved expression for R_o was established as

$$R_o = R_{oo} \left\{ 1 + \ln \left\{ 1 + \text{EXP}\left[\sum_{i=0}^{5} \beta_i (\ln\dot{\epsilon})^i \right] \right\} \right\}, \tag{37}$$

where $R_{oo} = q = 50$ KSI, $\beta_o = 48.88$, $\beta_1 = 18.30$, $\beta_2 = 2.767$, $\beta_3 = 0.2082$, $\beta_4 = 0.7813\text{x}10^{-2}$, and $\beta_5 = 0.1174\text{x}10^{-3}$.

---

*Contacts were made with ORNL to obtain the cyclic data from the tests reported in Refs. [2,5] but it was indicated that they were not available.

The revised material parameters of the extended Chaboche theory are listed in Table 3, and were employed to improve the material response predictions in Figs. 2 to 4.

IV. PREDICTIVE CAPABILITIES

The Chaboche theory has been employed to predict a wide range of additional mechanical behavior of Inconel 718 at 1200°F, including: strain-rate and strain-rate-history effects, creep and relaxation behavior, load-unload-reload behavior under strain or stress control, and strain-controlled, fully-reversed cyclic behavior.

Strain-Rate and Strain-Rate-History Effects

Three different strain rates; namely, $\dot{\epsilon}_1 = 5\text{x}10^{-5}\text{sec}^{-1}$, $\dot{\epsilon}_2 = 5\text{x}10^{-7}\text{sec}^{-1}$, $\dot{\epsilon}_3 = 5\text{x}10^{-9}\text{sec}^{-1}$, have been arbitrarily considered in studying the strain-rate effect. The stress-strain curves at these rates are shown in Fig. 5, which shows a rate dependency of initial yield that could not be predicted by the original Chaboche theory. This figure shows that the extended Chaboche theory predicts a pronounced strain rate effect for the strain rates considered. It is also noted that the stress-strain curves tend to be closer to each other as $\dot{\epsilon}$ increases. This behavior is consistent with the experiments, which have shown that an asymptotic behavior can eventually be reached.

A similar stress rate effect was predicted for three stress rates, obtained by multiplying the aforementioned strain rates by Young's modulus, as shown in Fig. 5. It is seen that the stress-controlled response overrides the strain-controlled response, the difference being attributed to the stress-strain nonlinearity of the constitutive equations.

The response of viscoplastic materials is significantly influenced by their strain rate history [24,26]. Perhaps the most useful and widely used experiment developed to study this behavior is the incremental (jump) test, where a specimen is first prestrained at one strain rate and then the strain rate is abruptly changed to another value. A material is said to exhibit a

strain-rate-history effect if the jump (interrupted) and monotomic (pure) responses remain distinct after significant strains have been imposed [21].

Let the constant strain rates before and after a jump be denoted $\dot{\epsilon}_1$ and $\dot{\epsilon}_2$, respectively, and let $\delta = \dot{\epsilon}_2/\dot{\epsilon}_1$; where $\delta > 1$ indicates a strain rate increase, $0 < \delta < 1$ corresponds to a strain rate decrease with increasing strain, and $\delta < 0$ implies strain rate reversal (unloading), Fig. 6. It can be shown that [27]

$$E_2^* = E - \frac{1}{\delta}(E - E_1^*) \quad , \tag{38}$$

where E_2^* and E_1^* are the slopes of the stress-strain curve immediately before and after the strain rate jump is imposed. If it is further assumed that $E_1^* \ll E$, it follows that $E_2^* \approx E$ for $\delta \gg 1$. In other words, the initial response after the strain rate increment is imposed is elastic, as experiments show. In case of stress-rate jumps, the analogue of Eq. (38) is

$$E_2^* = E\left[1 + \frac{1}{\gamma}\left(\frac{E}{E_1^*} - 1\right)\right]^{-1} \quad , \tag{39}$$

where $\gamma = \dot{\sigma}_2/\dot{\sigma}_1$ is the ratio of the stress rates [27].

Figure 7 shows the predicted monotonic responses at $\dot{\epsilon}_1 = 10^{-6}$ sec^{-1} and $\dot{\epsilon}_2 = 5\text{x}10^{-5}$ sec^{-1} as well as the corresponding interrupted responses for $\delta = 50$ (low-to-high strain rate) and $\delta = 0.02$ (high-to-low strain rate) after a prestrain of 0.75%.

For tensile loading, the saturation stress can be reached when each of the terms on the right hand side of Eq. (13) saturates. Numerical exercises with the Chaboche theory, however, have shown that R does not change substantially when small deformations, such as those produced during a tensile test, are considered, i.e., $R \approx R_o$. Thus, the hardening process is essentially kinematic, and, in the presence of recovery, the saturation value of Y is smaller than a and can be determined by solving Eq. (32). This equation shows that the saturation value of Y is solely dependent on the strain rate and is, therefore, strain-rate-history independent. The difference observed in predicted monotonic and interrupted behavior is, thus caused by different values of $R \approx R_o$ in the monotonic and jump tests. Since R_o increases with $\dot{\epsilon}$, the jump response lies below the uninterrupted

response for $\delta > 1$, i.e., the theory predicts a strain rate history effect typical of FCC materials [26]. Due to its treatment of R_o as a constant, the original Chaboche theory cannot predict strain-rate-history effects.

Prediction of the creep behavior of Inconel 718 at σ_h = 140 KSI, for load application rates of $\dot{\sigma}_1$ = 20 KSI/sec and $\dot{\sigma}_2$ = 0.20 KSI/sec, are presented in Fig. 8. In each case, the response from the moment of loading until the stress reached its hold value was predicted as well as the response for an additional 300 sec, with only the creep strains shown in Fig. 8. It was found that the creep strain corresponding to the higher stress rate overrides that corresponding to the lower rate. However, the total strain (not shown in Fig. 8) in the latter case was greater. This was expected, since at the lower stress rate, yielding initiated at a stress value much lower than σ_h = 140 KSI and by the time the stress value reached the hold value substantial hardening had already taken place. Thus, the material was capable of sustaining further deformations only at lower rates. These results suggest the importance of specifying the rate of load application, in addition to the hold stress, when reporting creep data.

When steady-state creep is reached, Eq. (13) yields upon differentiation with respect to time

$$\dot{Y} - \dot{R} = 0 , \qquad \text{or} \qquad \dot{Y} = \dot{R} . \tag{40}$$

For tensile creep, $\dot{Y}$ is positive, and Eq. $(40)_b$ is valid only if $\dot{R}$ is negative, i.e., when the material undergoes isotropic softening. Numerical solutions have shown that Inconel 718 at 1200°F starts to harden kinematically and soften isotropically with the initiation of creep deformations, with the rate of hardening being higher than the softening rate. However, a point is eventually reached where both rates are equal in magnitude. At this point Eq. $(40)_b$ is satisfied and thereafter softening begins to dominate, thus allowing for increasing strain rates, as Fig. 9 depicts for creep at 125 KSI. As mentioned earlier, there is experimental evidence that the increasing creep rates, at least in early stages, are not a manifestation of instability or impending failure [3,6]. Therefore, it is concluded that the Chaboche theory can predict realistic creep behavior,

including increasing creep rates following steady-state creep, caused by material softening.

Relaxation Behavior

In a stress relaxation situation, Eqs. (6) and (7) give

$$\dot{\sigma} = - E\dot{\epsilon}'' \cdot \tag{41}$$

If the stress relaxes from a positive value, $\dot{\epsilon}''$ is initially positive and $\dot{\sigma}$ is, therefore, negative. Experimental data on metals and alloys show that the stress normally relaxes at a decreasing rate until a steady state is eventually reached when $\dot{\sigma} = 0$, i.e., when

$$\sigma = Y + R \cdot \tag{42}$$

To examine the stress relaxation prediction of the Chaboche theory, a loading history was chosen, which consisted of straining at a rate of $5\text{x}10^{-5}$ sec^{-1} to 1% strain. The strain was then held at this value for 50 minutes. The results are shown in fig. 10, and are consistent with the above discussion.

Load-Unload-Reload Behavior

A reversal in strain (stress) corresponds to an instantaneous jump in $\dot{\epsilon}(\dot{\sigma})$ with $\delta(\gamma) < 0$. Three different cases can be distinguished (c.f. Fig.6): (a) $\delta(\gamma) = -1$, which corresponds to a reversal with constant strain (stress) rate magnitude, (b) $\delta(\gamma) << -1$, which represents a large increase in the strain (stress) rate magnitude, and (c) $1/\delta(\gamma) << -1$, which represents a large decrease in strain (stress) rate magnitude upon unloading.

The loading-unloading behavior of Inconel 718 at 1200°F is now studied under strain (stress) control in a fashion similar to that of Ref. [28]. For strain control, a loading rate of $\dot{\epsilon}_o = 5\text{x}10^{-7}$ sec^{-1} was arbitrarily selected, along with unloading rates of $\dot{\epsilon}_1 = -5\text{x}10^{-5}$ sec^{-1} ($\delta_1 = -10^2 << -1$), $\dot{\epsilon}_2 = -5\text{x}10^{-7}$ sec^{-1} ($\delta_2 = -1$), $\dot{\epsilon}_3 = -5\text{x}10^{-9}$ sec^{-1} ($\delta_3 = -10^{-2}$, or $1/\delta_3 = -10^2 << -1$). In each case, unloading was initiated after a strain of 0.75% was reached,

where $E_1^* \ll 1$, as was assumed in deriving Eq. (38). The results are shown in Fig. 11, where it is seen that the initial unloading behavior is inelastic and is sensitive to δ. For a large increase in the strain rate magnitude at reversal, the terms with $1/\delta$ in Eq. (38) are negligible and $E_2^* \approx E$, i.e., the initial unloading response is elastic, which is in agreeement with the predicted behavior shown in Fig. 11 for $\delta_1 = -10^{-2}$. For $\delta_2 = -1$, Eq. (38) gives $E_2^* = 2E$, which means that the initial unloading response is inelastic. Figure 11 however, shows that the slope very rapidly approximated E as the stress decreased. For large decreases in strain rate magnitudes at reversal, the terms with $1/\delta$ dominate and $E_2^* \approx E/|\delta|$. Therefore, significant inelastic unloading response with a very large positive slope was predicted, resulting in near-vertical decay of the stress at the start of unloading. The inelastic strain increased when $\delta_3 = -10^{-2}$ was imposed, and can be thought of as stress relaxation, since the stress decreases at almost constant strain.

For stress control, the stress rates were obtained by multiplying the prior strain rates by E. In each case, the loading period was adjusted so that a strain of 1% was obtained before unloading was started. The results are shown in Fig. 12. For $\gamma \ll -1$, Eq. (39) yields a value of $E_2^* = E$, i.e., the initial unloading response is elastic, as Fig. 12 depicts for $\gamma_1 = -10^2$. For $\gamma_2 = -1$, the initial slope upon unloading can be found from Eq. (45) to be $E_2^* = -E_1^*$, i.e., the initial unloading response is inelastic with a negative slope that is equal in magnitude to the slope before unloading. As the stress decreases, however, the unloading response approaches a linear shape typical of elastic unloading, as shown in Fig. 12. For $1/\gamma \ll -1$, Eq. (39) reduces to $E_2^* = -|\gamma| E_1^*$. Consequently, the initial unloading slope is negative and much smaller in magnitude than the slope before unloading. The theory, therefore, predicts significant inelastic unloading behavior with small decreases in stress and very large increases in inelastic strain, as shown in Fig. 12, for $\gamma_3 = -10^{-2}$. This latter case is analogous to a creep test, where the stress is held almost constant while the strain increases substantially.

The analysis was further expanded by studying the effect of unloading rate on subsequent reloading behavior. Two cases were considered: (a) loading, unloading, and reloading at $|\dot{\epsilon}| = 5 \times 10^{-5} \text{sec}^{-1}$, and (b) loading and

reloading at $\dot{\epsilon}_1$ and unloading at $\dot{\epsilon}_2 = -5\text{x}10^{-7}\text{sec}^{-1}$. In each case, loading was applied until a strain of 0.75% was reached, unloading was initiated and maintained to a strain of 0.45%, and finally loading was continued to a strain of 1.0%. The results are shown in Fig. 13 for both cases. In the first case ($\delta = -1$ at unloading), the initial slope upon unloading is positive and twice the elastic response, i.e., the initial response is inelastic. However, it rapidly approximates the linear elastic response and, therefore, the reloading response immediately approaches the monotonic response at the loading rate. In the second case ($\delta = -10^{-2}$ at unloading), however, significant inelastic deformations occurred upon unloading and the consequent reloading response at $\dot{\epsilon}_1$ was considerably different from the monotonic response at the same rate. Note that differences in reloading behavior in the two cases are due essentially to the amount of inelastic deformations that occurred upon unloading. It is possible to conclude, therefore, that the Chaboche theory is capable of simulating a history-dependent reloading response that memorizes rate-dependent prior deformations.

Cyclic Softening

As mentioned earlier, Inconel 718 at 1200°F undergoes cyclic softening for approximately 10-20 % of its fatigue life. In Chaboche's theory, cyclic softening is modeled by the isotropic hardening variable R, with its saturation value q smaller than its initial value R_o. The first few hysteresis loops of a strain-controlled, fully-reversed cyclic test at $|\dot{\epsilon}| = 4\text{x}10^{-5}$ sec^{-1} and $\Delta\epsilon = 2\%$ were predicted and are shown in Fig. 14. In this figure, cyclic softening is manifested by a continuous decrease in the stress range and a corresponding increase in the inelastic strain range with cycling.

V. CONCLUSIONS

The modified Chaboche theory of viscoplasticity has been employed to model the viscoplastic behavior of Inconel 718 at 1200°F. A procedure has been developed and used for the determination of the material parameters of this theory from available uniaxial experimental data of standard mechanical

tests. The procedure for determining the parameters is not unique, but is considered appropriate for the available data, which were not adequate for the purpose of evaluating the Chaboche material parameters.

The sensitivity study undertaken herein has resulted in an 'optimal' set of material parameters, which gave better overall agreement between theory and prediction. The study has also emphasized the influence of each material parameter on different aspects of material behavior.

The predictive capabilities of the theory have been demonstrated for a variety of uniaxial loading conditions. The lack of adequate data base, however, precludes drawing detailed conclusions about the accuracy of the predicted behavior. Nonetheless, the Chaboche theory appears to offer a considerable promise for successfully modeling viscoplastic material behavior.

ACKNOWLEDGMENT - The authors thank Dr. T. Nicholas of the AFWAL Materials Laboratory, Wright-Patterson Air Force Base, for his technical assistance in providing experimental data for Inconel 718 at 1200°F.

VI. REFERENCES

1. Barker, J.F., Ross, E.W., and Radavich, J.F., "Long Time Stability of INCONEL 718," Journal of Metals, pp. 31-41, January 1970.

2. Brinkman, C.R., and Korth, G.E., "Strain Fatigue and Tensile Behavior of Inconel 718 from Room Temperature to 650°C," Journal of Testing and Evaluation, JTEVA, Vol. 2, No. 4, pp. 249-259, 1984.

3. Booker, M.K., "An Interim Analytical Representation of the Creep Strain-Time Behavior of Commercially Heat Treated Alloy 718," ORNL/TM 6232, 1978.

4. Domas, P.A., Sharpe, W.N., Ward, M., and Yau, J., "Benchmark Notch Test for Life Prediction," Technical Report Submitted to NASA under contract NAS3-22522, 1982.

5. Korth, G.E., and Smolik, G.R., "Status Report of Physical and Mechanical Test Data of Alloy 718," TREE 1254, 1978.

6. Booker, M.K., "Progress Toward Analytical Description of the Creep Strain-Time Behavior of Engineering Alloys," CONF 800907-2, 1980.

7. Wilson, D.A., and Walker, K.P., "Constitutive Modeling of Engine Materials," AFWAL-TR-84-4073, 1984.

8. Beaman, R.L., "The Determination of the Bodner Material Coefficients for IN 718 and Their Effects on Cyclic Loading," M.S. Thesis, Air Force Institute of Tehcnology, 1984.

9. Nicholas, T., Private Communication.

10. Abdel-Kader, M.S., "A Comparative Study of the Chaboche and Bodner Theories of Viscoplasticity for High Temperature Applications," D.Sc. Dissertation, The George Washington University, Washignton, D.C., 1986.

11. Booker, M.K., and Sikka, V.K., "A Study of Tertiary Creep Instability in Several Elevated-Temperature Structural Materials," Thechnical Report Submitted to the Division of Reactor Research and Technology, U.S. Department of Energy under Contract W-7405-eng-26, 1979.

12. Chaboche, J.L., "Viscoplastic Constitutive Equations for the Description of Cyclic and Anistotropic Behavior of Metals," Bulletin De L'Academie Polanaise des Sciences, Vol. 25, No. 33, 1977.

13. Chaboche, J.L., and Rousselier, G., "On the Plastic and Viscoplastic Constitutive Equations - Part I: Rules Developed With Internal Variable Concept," J. Pressure Vessel Tech., Vol. 105, pp. 153-158, 1983.

14. Chaboche, J.L., "Thermodynamic and Phenomenological Description of Cyclic Viscoplasticity With Damage," Translation of Publication No. 1978-3 of the Office National d'Etudes et de Researches Aerospatiales, France, by the European Space Agency Technical Translation Service, Publication No. ESA-TT-548, 1979.

15. Chaboche, J.L., et al, "Modelization of the Strain Memory Effects on the Cyclic Hardening of 316 Stainless Steel," in Fifth Int. Conference on Structural Mechanics in Reactor Technology, Berlin, W. Germany, 1979.

16. Chaboche, J.L., and Rousselier, G., "On the Plastic and Viscoplastic Constitutive Equations - Part II: Application of Internal Variable Concepts to the 316 Stainless Steel," J. Pressure Vessel Tech., Vol. 105, pp. 159-164, 1983.

17. Eftis, J., and Jones, D.L., "Life Prediction for a Structural Material Under Cyclic Loads With Hold Times Using a Viscoplastic Constitutive Model," Final Technical Report, Air Force Office of Scientific Research, Washington, D.C., U.S.A., 1983.

18. Chiu, S.S., Eftis, J., and Jones, D.L., "Application of Cyclic Viscoplastic Theory to Low Cycle Fatigue Life Prediction of Ti-6Al-4V," Proc. NUMETA' 85 Conference, Swansea, U.K., 7-11 January, 1985.

19. Abdel-Kader, M.S., Eftis, J., Jones, D.L., "An Extension of the Chaboche Theory of Viscoplasticity to Account for Rate-Dependent Initial Yield," SECTAM XIII, Columbia, South Carolina, 1986.

20. Eftis, J., and Jones, D.L., "Evaluation and Development of Constitutive Relations for Inelastic Behavior," Final Technical Report, Air Force Office of Scientific Research, Washington, D.C., U.S.A., 1983.

21. Haisler, W.E., and Imbire, P.K., "Numerical Considerations in the Development and Implementation of Constitutive Models," NASA Second Symposium on Nonlinear Constitutive Relations for High Temperature Applications," NASA Lewis Research Center, Clev., Ohio, 1984.

22. Draper, N.R., and Smith, H., "Applied Regression Analysis," J. Wiley, pp. 263-304, 1966.

23. Stouffer, D.C., "A Constitutive Representation for IN 100," Technical Report AFWAL-TR-81-4039, 1981.

24. Lindholm, U.S., "Some Experiments With Split Hopkinson Pressure Bar," J. Mech. Phys. Solids, Vol. 12, pp. 317-335, 1964.

25. Eleiche, A.M., and Campbell, J.K., "The Influence of Strain Rate History and Temperature on the Shear Strength of Copper, Titanium, and Mild Steel, "Technical Report AFML-TR-76-90, 1976.

26. Duffy, J., "Strain Rate History Effects and Dislocation Substructure at High Strain Rates," in Mechanical Behavior Under High Stress and Ultrahigh Loading Rates, Ed. by J. Mescall and V. Weiss, Plenum Publishing Corporation, 1983.

27. Cernocky, E.P., "An Examination of Four Viscoplastic Constitutive Theories in Uniaxial Monotonic Loading," Int. J. Solids Structures, Vol. 18, No. 11, pp. 989-1005, 1982.

28. Cernocky, E.P., "Comparison of the Unloading and Reversed Loading Behavior of Three Viscoplastic Constitutive Theories," Int. J. Nonlinear Mechanics, Vol. 17, No. 4, pp. 255-266, 1982.

Table 1: Values of K^*, n^*, a, and c for Inconel 718 at 1200°F

Ser. No.	Ref.	Test	Strain Rate, $\dot{\epsilon}$ Sec^{-1}	No. of Data Points	K^* KSI	n^*	a KSI	c
1	4	cyclic	8.333×10^{-4}	4	202.3	0.1080	24.46	364.4
2	4	cyclic	3.333×10^{-3}	3	188.7	0.1100	31.81	347.0
3	4	cyclic	1.667×10^{-2}	4	156.6	0.0920	33.86	349.0
4	5	cyclic	4.000×10^{-3}	12	188.2	0.1078	31.49	349.1
5	2	cyclic	4.000×10^{-3}	37	172.2	0.1017	28.13	355.0
6	2,5	cyclic	4.000×10^{-3}†	49	187.9	0.1096	31.64	347.5
7	9	cyclic	2.667×10^{-3}†	3	214.9	0.1562	39.97	301.5
8	4	tensile	1.670×10^{-4}		166.9	0.0540	----	----
9	4	tensile	3.330×10^{-5}		210.0	0.0630	----	----

†Some tests were performed at $\dot{\epsilon} = 10^{-4}$ sec^{-1} and 10^{-5} sec^{-1}

Table 2: Calculation of R and p for the determination of b and q

Cycle No.	σ KSI	ϵ''_a† %	p	Y KSI	R KSI
1	115.0	0.530	0.0265	28.57	39.04
4	109.8	0.546	0.0907	28.71	33.32
8	105.4	0.561	0.1568	28.84	28.83
12	102.4	0.561	0.2247	28.95	25.72
16	101.0	0.588	0.2942	29.04	24.25
20	99.42	0.588	0.3648	29.04	22.66
24	98.43	0.588	0.4354	29.04	21.67
28	97.43	0.588	0.5059	29.04	20.67
32	95.44	0.591	0.5766	29.06	18.66
36	95.44	0.596	0.6477	29.09	18.63
40	95.44	0.596	0.7192	29.09	18.63

†Inelastic strain amplitude, $\Delta\epsilon''/2$

Table 3: Material parameters of Chaboche's theory, Inconel 718 at 1200°F

Parameter	Description	Initial Value	Optimal Value
E	Young's modulus	24.73×10^{-3}	24.73×10^{-3}
ν	Poisson's ratio	0.3356	0.3356
a	Saturation value of kinematic hardening variable	31.40	30.00
c	Kinematic hardening exponent	349.5	350.0
γ	Coefficient of recovery	0.4×10^{-10}	0.4×10^{-10}
m	Recovery exponent	6.942	7.000
K	Overstress parameter	154.4 KSI$\sqrt[n]{\text{sec}}$	155.0 KSI$\sqrt[n]{\text{sec}}$
n	Strain rate sensitivity parameter	5.120	5.100
q	Saturation value of isotropic hardening variable	18.62 KSI	50.00 KSI
b	Isotropic hardening exponent	4.679	3.75
R_o	Initial, rate-dependent value of isotropic hardening	Eq.(31)	Eq.(37)

Table 4: Effect of changing n by ±(3.5, 7.0)% on tensile behavior, Inconel 718 at 1200°F

Strain Rate Sec^{-1}	Saturation Stress, KSI					
	Exper.	Predictions				
		0.930n	0.965n	n	1.035n	1.70n
1.1×10^{-6}	134	128.28	129.20	130.18	131.12	132.33
1.3×10^{-5}	142	143.57	144.85	146.23	147.62	148.90

Table 5: Effect of changing R_o by $\pm$(1.75, 3.5, 5.25, 7.0)% on creep behavior, Inconel 718 at 1200°F

Hold Stress KSI	Minimum Creep Rate, Sec^{-1}									
	Exper.	Predictions								
		$0.930R_o$	$0.9475R_o$	$0.965R_o$	$0.985R_o$	R_o	$1.0175R_o$	$1.035R_o$	$1.0525R_o$	$1.070R_o$
80	4.0×10^{-9}	4.519×10^{-8}	2.668×10^{-8}	1.503×10^{-8}	8.038×10^{-9}	3.991×10^{-9}	1.853×10^{-9}	9.831×10^{-10}	7.119×10^{-10}	7.004×10^{-10}
100	1.6×10^{-8}	4.250×10^{-7}	2.706×10^{-7}	1.660×10^{-7}	9.828×10^{-8}	5.533×10^{-8}	2.944×10^{-8}	1.470×10^{-8}	7.518×10^{-9}	1.209×10^{-8}
110	3.0×10^{-8}	5.519×10^{-7}	3.374×10^{-7}	1.984×10^{-7}	1.113×10^{-7}	5.898×10^{-8}	2.917×10^{-8}	1.325×10^{-8}	9.232×10^{-9}	9.048×10^{-9}
120	1.5×10^{-7}	1.141×10^{-6}	7.052×10^{-7}	4.200×10^{-7}	2.394×10^{-7}	1.295×10^{-7}	6.591×10^{-8}	3.441×10^{-8}	2.245×10^{-8}	2.806×10^{-8}
125	3.5×10^{-7}	2.253×10^{-6}	1.439×10^{-6}	8.931×10^{-7}	5.331×10^{-7}	3.058×10^{-7}	1.667×10^{-7}	8.627×10^{-8}	4.955×10^{-8}	6.433×10^{-8}
130	8.3×10^{-7}	5.119×10^{-6}	3.418×10^{-6}	2.228×10^{-6}	1.413×10^{-6}	8.674×10^{-7}	5.127×10^{-7}	2.898×10^{-7}	1.584×10^{-7}	1.171×10^{-7}
135	5.5×10^{-6}	1.139×10^{-5}	7.863×10^{-6}	5.345×10^{-6}	3.558×10^{-6}	2.311×10^{-6}	1.459×10^{-6}	8.916×10^{-7}	5.244×10^{-7}	3.804×10^{-7}
140	7.0×10^{-6}	2.129×10^{-5}	1.509×10^{-5}	1.051×10^{-5}	7.198×10^{-6}	4.834×10^{-6}	3.172×10^{-6}	2.023×10^{-6}	1.254×10^{-6}	1.126×10^{-6}

Table 6: Effect of changing material parameters by values ranging from ±1.75% to ±7.0% on cyclic behavior[1], Inconel 718 at 1200°F

Parameter	0.930P[2]		0.9475P		0.9650P		0.9825P		P		1.0175P		1.0350P		1.0525P		1.070P	
	$\Delta\sigma_1$ KSI	$\Delta\epsilon_1^{in}$ %	$\Delta\sigma_1$ KSI	$\Delta\epsilon_1^{in}$ %	$\Delta\sigma_1$ KSI	$\Delta\epsilon_1^{in}$ %	$\Delta\sigma_1$ KSI	$\Delta\epsilon_1^{in}$ %	$\Delta\sigma_1$ KSI	$\Delta\epsilon_1^{in}$ %	$\Delta\sigma_1$ KSI	$\Delta\epsilon_1^{in}$ %	$\Delta\sigma_1$ KSI	$\Delta\epsilon_1^{in}$ %	$\Delta\sigma_1$ kSI	$\Delta\epsilon_1^{in}$ %	$\Delta\sigma_1$ kSI	$\Delta\epsilon_1^{in}$ %
a	307.5	0.753	---	---	---	---	---	---	309.6	0.745	---	---	---	---	---	---	311.5	0.737
c	308.6	0.749	---	---	---	---	---	---	"	"	---	---	---	---	---	---	310.4	0.742
γ	309.7	0.744	---	---	---	---	---	---	"	"	---	---	---	---	---	---	309.4	0.747
m	312.0	0.735	---	---	311.0	0.739	---	---	"	"	---	---	307.7	0.753	---	---	305.7	0.761
K	306.7	0.758	---	---	308.2	0.751	---	---	"	"	---	---	311.1	0.740	---	---	312.4	0.733
n	303.9	0.768	---	---	306.7	0.757	---	---	"	"	---	---	312.4	0.734	---	---	315.2	0.722
b	310.0	0.743	---	---	---	---	---	---	"	"	---	---	---	---	---	---	309.2	0.747
q	309.5	0.745	---	---	---	---	---	---	"	"	---	---	---	---	---	---	309.7	0.745
R_o[3]	294.3	0.808	298.2	0.793	302.0	0.777	305.8	0.761	"	"	313.4	0.730	317.2	0.714	320.9	0.699	324.7	0.689

1/ Experimental values : $\Delta\sigma_1$ = 285 KSI, $\Delta\epsilon_1^{in}$ = 0.83%.
2/ P refers to any of Chaboche's parameters.
3/ R_o = 115.5 KSI for $\dot{\epsilon}$ = 4×10^{-6} sec^{-1}, Eq. (31).

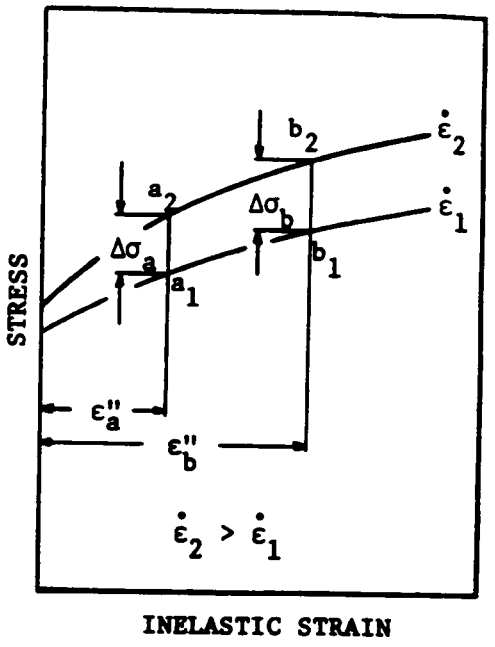

Fig. 1. Illustration of two stress-inelastic strain curves at different strain rates.

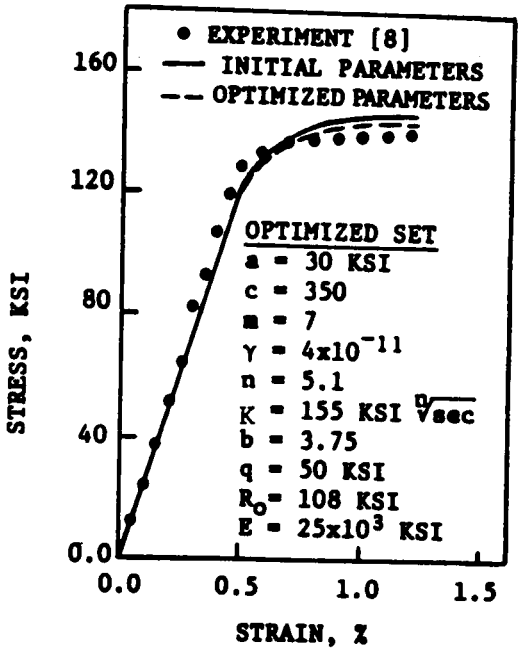

Fig. 2. Comparison of experimental and predicted monotonic response at $\dot{\varepsilon} = 1.333 \times 10^{-5} sec^{-1}$.

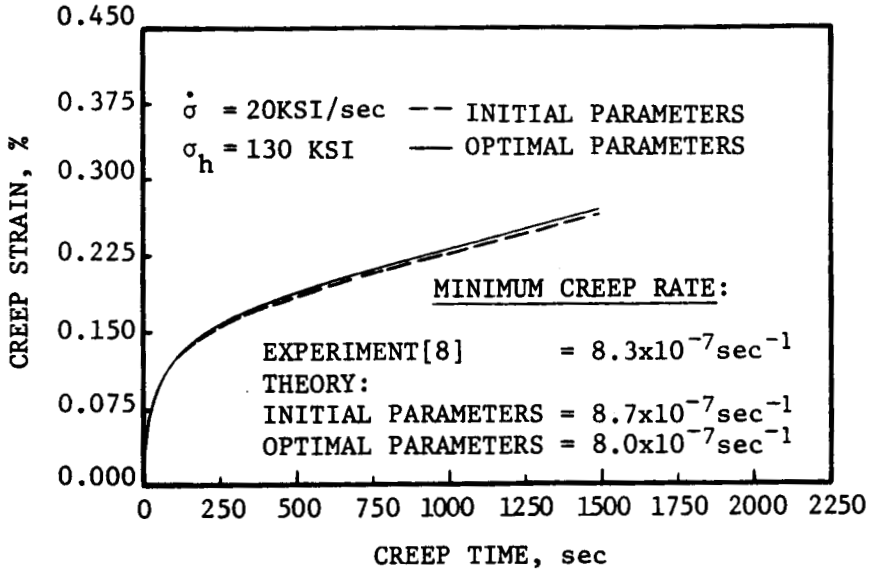

Fig. 3. Predicted creep response at $\sigma_h = 130$ KSI; only experimental steady state is available.

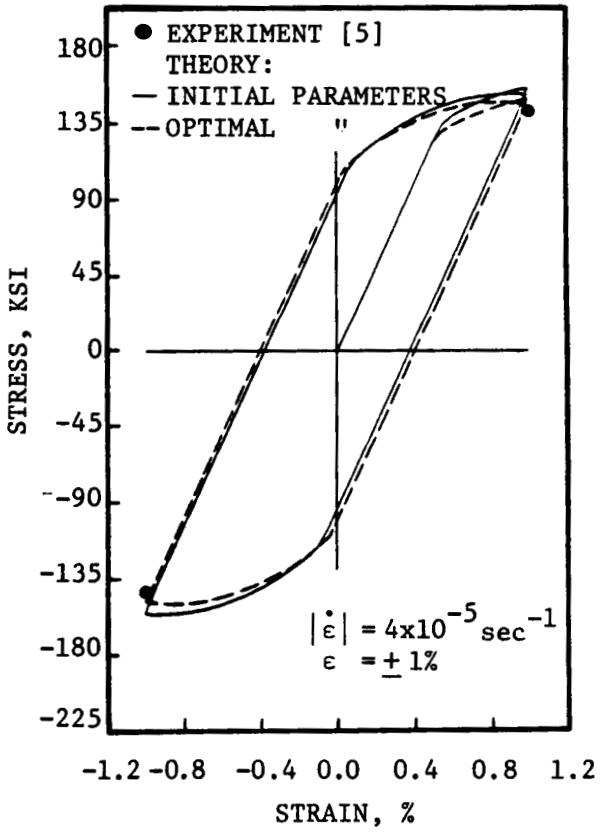

Fig. 4. Predicted cyclic response at $|\dot{\varepsilon}| = 4\times10^{-5}\text{sec}^{-1}$ and $\varepsilon = \pm 1\%$; only experimental peak stresses are available.

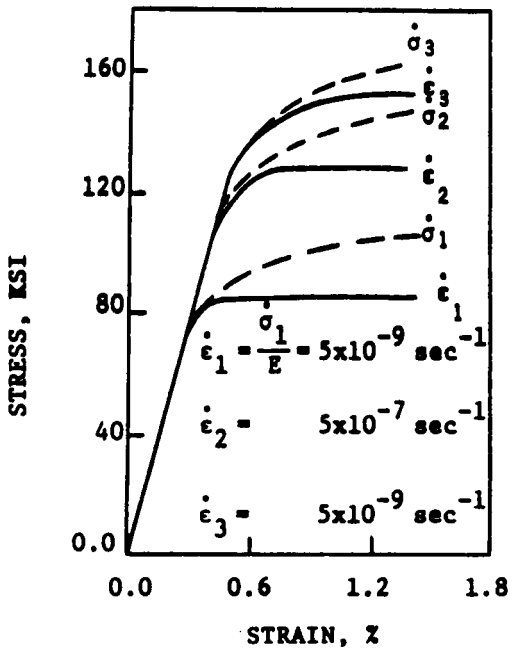

Fig. 5. Predicted stress-strain response at different strain and stress rate.

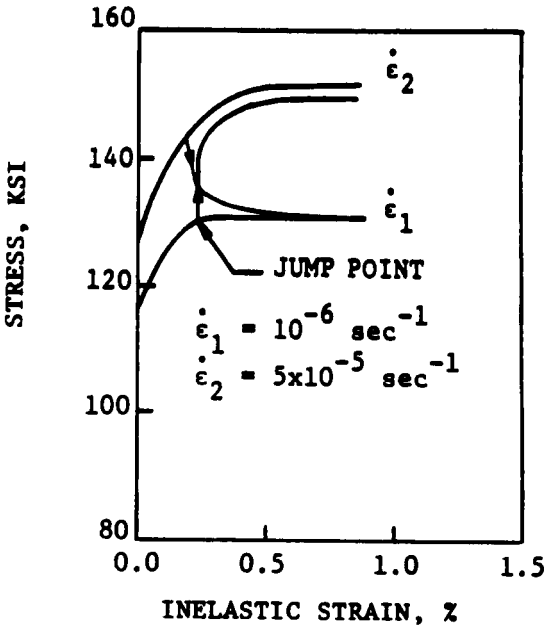

Fig. 7. Predicted monotonic and interruped responses at different strain rates.

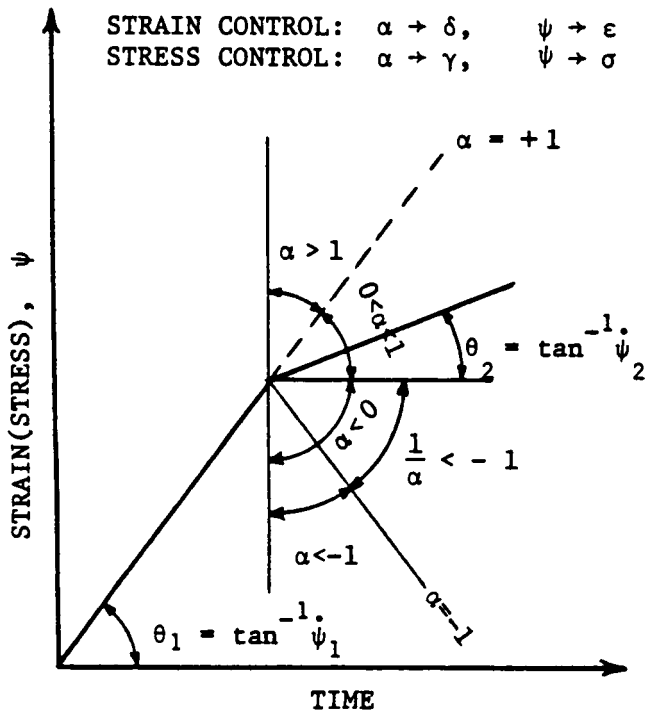

Fig. 6. Illustration of strain (stress) rate changes.

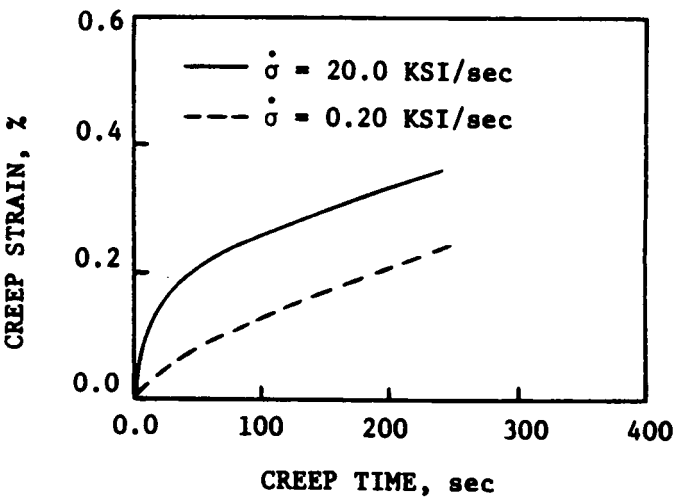

Fig. 8. Predicted creep response at $\sigma_h = 140$ KSI for different loading rates.

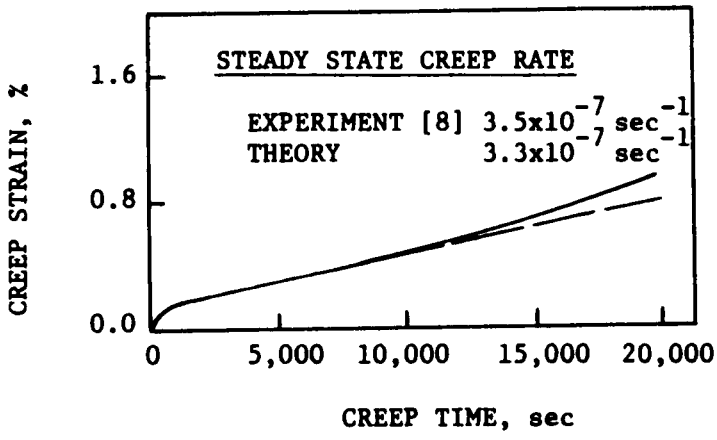

Fig. 9. Predicted creep response at $\sigma_h = 125$ KSI and $\dot{\sigma} = 20$ KSI/sec.

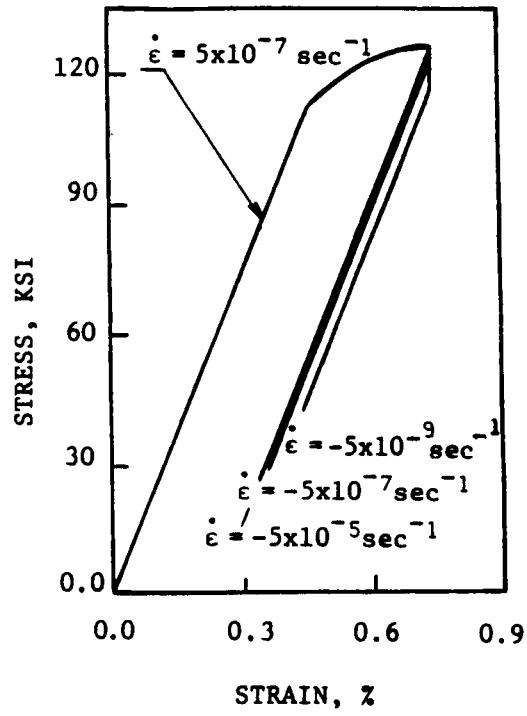

Fig. 11. Predicted load-unload response at different unloading strain rates.

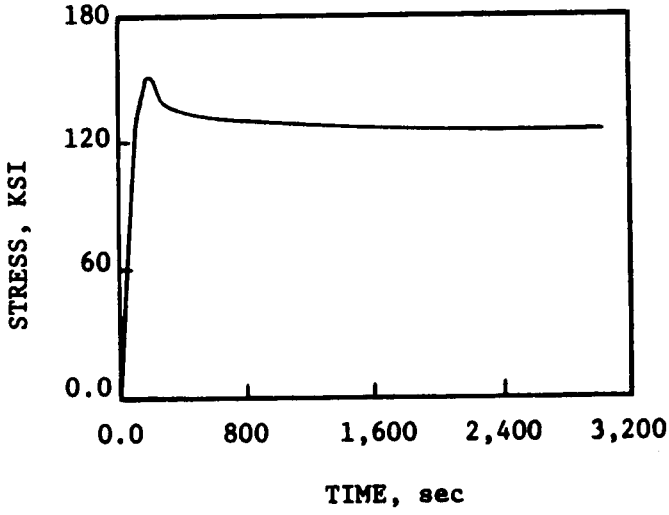

Fig. 10. Predicted relaxation response at $\varepsilon = 1\%$

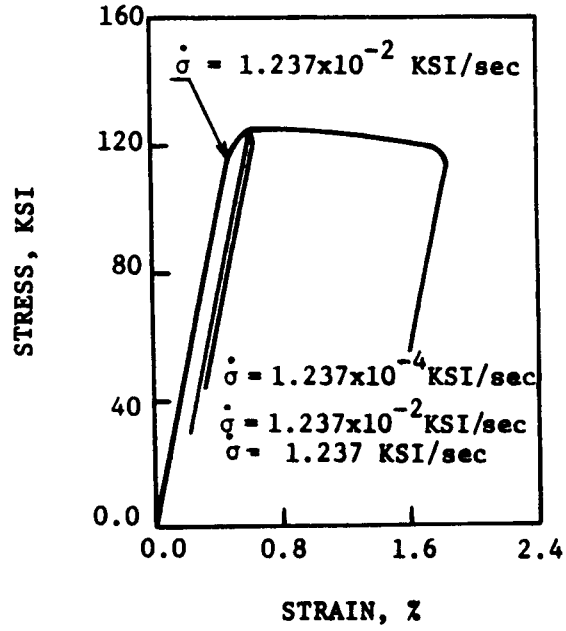

Fig. 12. Predicted load-unload response at different unloading stress rates.

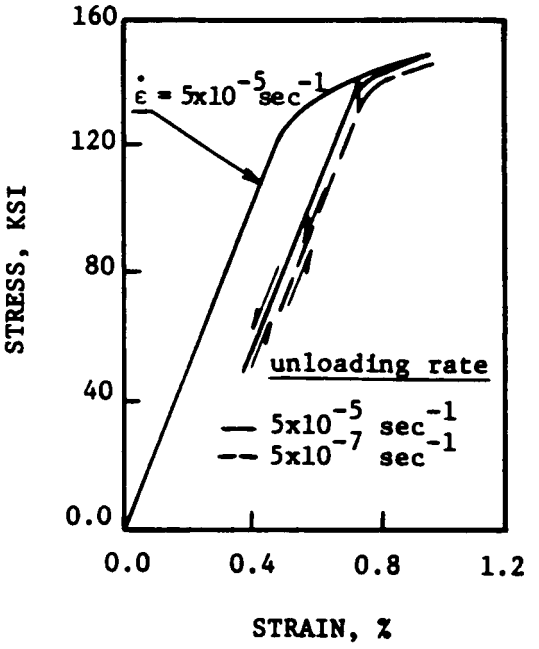

Fig. 13. Predicted load-unload-reload response at different unloading strain rates.

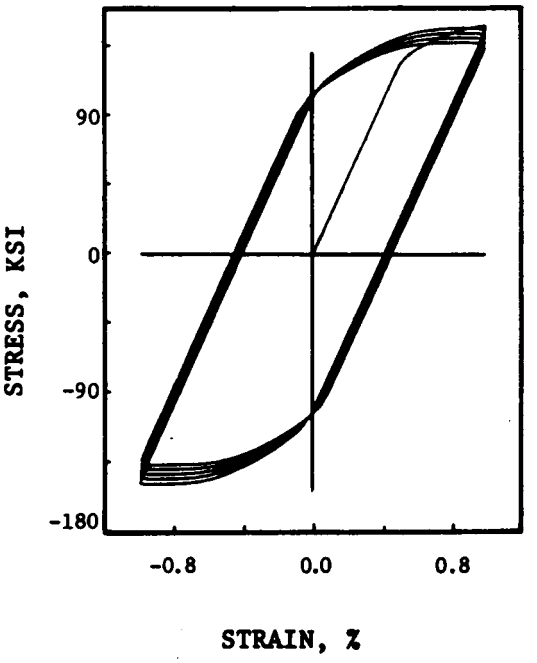

Fig. 14. Predicted cyclic response at $|\dot{\varepsilon}|$ = 4x10^{-5}sec^{-1} and $\varepsilon = \pm 1\%$.